International Journal of Mass Spectrometry 275 (2008) 91–103

Contents lists available at ScienceDirect

International Journal of Mass Spectrometry

journal homepage: www.elsevier.com/locate/ijms

Dipole excitation of ions in linear radio frequency quadrupole ion traps with added multipole fields

XianZhen Zhao*, D.J. Douglas

Department of Chemistry, University of British Columbia, Vancouver, BC, Canada

ARTICLE INFO

Article history:
Received 25 February 2008
Received in revised form 16 May 2008
Accepted 19 May 2008
Available online 3 June 2008

Keywords:
Linear ion trap
Higher order multipole
Ion excitation
Nonlinear resonance

ABSTRACT

Ion motion with auxiliary dipole excitation and collisional damping in a linear radiofrequency quadrupole ion trap incorporating small amounts of even higher order multipoles is studied analytically. The ion motion is modeled in a pseudopotential that is mostly quadratic with small amounts of higher spatial harmonics. Ion motion along x and y axes is characterized by two uncoupled forced and damped anharmonic oscillator equations. A multiple time scales method is used to solve the equations of motion of ions with a first order perturbation correction. Analytical relations between the oscillation amplitudes at steady state (the stationary amplitudes) and excitation frequency are calculated. The frequency response curves show that in some cases bistable behavior might be obtained, i.e., there are two stable stationary amplitudes for a given excitation frequency.

1. Introduction

Practical quadrupole rf ion traps, either 3D traps with hyperbolic electrodes or 2D linear ion traps with four parallel electrodes, have distortions to the field. These distortions are introduced by the truncation of the electrodes, the use of round rather than hyperbolic electrodes, and possible construction errors in the electrode spacings or geometries. Field distortions add small nonlinear electric field components to the linear field of the quadrupole in the trapping region. For a linear quadrupole, the potential with distortions can be written as a weighted sum of multipoles [1]:

$$\Phi(x_r, y_r) = \mathrm{Re}\left[\sum_{n=0}^{\infty} A_n \left(\frac{x_r + iy_r}{r_0}\right)^n\right] \tag{1}$$

with a time dependent potential

$$V(x_r, y_r, t_r) = [U - V_{\mathrm{rf}} \cos(\Omega t_r + \varphi_0)]\Phi(x_r, y_r), \tag{2}$$

where A_n is the dimensionless amplitude of a multipole, x_r, y_r are Cartesian coordinates, t_r is time, U is an applied dc voltage, V_{rf}, Ω, and φ_0 are the zero to peak amplitude, the angular frequency, and the initial phase of an applied rf voltage, and r_0 is the field radius of the quadrupole. Re[F] is the real part of the function $F(x_r + iy_r)$, and $i^2 = -1$. Analytical expressions for the multipoles are given by Szilagyi [2].

The performance of an ion trap or a mass filter can be improved by deliberately introducing and controlling suitable multipole fields. For instance, a 3D ion trap with infinite hyperbolic electrodes that satisfy the condition $r_0 = \sqrt{2}z_0$, where r_0 and z_0 are distances from the trap center to the ring and end cap electrodes respectively, generates a quadrupole field at the center of the ion trap. However, the truncation of the electrodes for a practical ion trap results in the addition of a negative octopole (relative to the quadrupole field), which delays ion ejection during mass selective instability scans [3]. Both the stretched geometry [4] and the modified hyperbolic angle [5]3D ion traps were introduced to counteract the deleterious effects of the octopole. With these changes, a larger positive octopole field is introduced in these ion traps [6]. This added octopole field can lead to faster ion ejection, either at a stability boundary [7,8] or with resonant excitation [9], to give higher resolution with mass selective instability scans [3]. Miniature ion traps, such as rectilinear ion traps [10], cylindrical ion traps

* Corresponding author.
E-mail address: xzhao@chem.ubc.ca (X. Zhao).

1387-3806/$ – see front matter.
doi:10.1016/j.ijms.2008.05.034

[11], and the halo ion trap [12], also have higher order multipoles in their trapping regions. For a linear quadrupole mass filter constructed with round rods, improved peak shape is achieved by choosing a ratio of rod radius to field radius that properly balances the amplitudes A_6 and A_{10} [13,14], rather than making the amplitude A_6 zero [15].

Higher order fields present in 3D ion traps [16] and linear traps can increase fragmentation efficiency. Collings et al. observed relatively high MS/MS efficiency with a linear quadrupole trap operated at a pressure of 3.5×10^{-5} Torr, and attributed this to the higher multipoles present in the field of a round rod quadrupole compared to a quadrupole with an ideal field [17]. Collings also showed that a dc octopole field added with auxiliary electrodes can improve MS/MS efficiency [18]. Michaud et al. [19] showed that adding a 4% octopole field (i.e., $A_4/A_2 = 0.04$) to a linear quadrupole can substantially improve fragmentation efficiency for MS/MS, especially at pressures of 10^{-4} Torr or less of N_2.

Sudakov and Douglas [20] showed a small amplitude octopole field can be added to a linear quadrupole constructed with round rods by making one pair of the electrodes larger in diameter than the other pair, with all rods equally spaced from the central axis. Later Konenkov et al. [21] described methods of adding a hexapole field to a linear quadrupole constructed with round rods. These methods also add other higher multipoles to the potential.

The presence of a higher multipole field in an ion trap introduces nonlinear ion dynamics. For instance, the ion motion with dipolar excitation and collisional damping is like that of a damped and forced anharmonic oscillator. The oscillation frequency depends on the oscillation amplitude. This can result in a multivalued dependence of the oscillation amplitude on the excitation frequency [22,23]. For some excitation frequencies, there may exist more than one amplitude. When two stable amplitudes exist for one excitation frequency, we refer to this as *bistability*. If the excitation frequency is scanned, sudden large changes in ion oscillation amplitude may occur. The frequencies, at which such "jumps" in amplitude occur depend on the frequency scanning directions [23,24]. When the excitation is applied at discrete frequencies and is not scanned [19], the frequency where a jump in amplitude occurs is not easily determined. However, large jumps in amplitude with small changes in excitation frequency are still possible for discrete excitation frequencies [19]. In principle, these sudden jumps can be used to produce high mass resolution in isolating ions [25].

The addition of a hexapole or octopole field to a linear quadrupole adds cubic or quartic terms to the potential. As discussed by Konenkov et al. [21] and Michaud et al. [19] respectively, analytical expressions given by Landau and Lifshitz can be used to calculate the frequency shifts caused by the added multipoles in these cases. Michaud et al. noted that several authors have stated that field distortions in 3D traps can cause shifts of the ion oscillation frequency [26–29] but in general the magnitude or signs of the shifts were not related to the multipole amplitudes. Sevugarajan and Menon [30] calculated the frequency shifts of the z motion in 3D traps with added hexapole or octopole fields for the case where there is no damping, and derived the formula given by Landau and Lifshitz. The frequency shifts in quadrupole ion traps caused by multipole fields higher than an octopole, or combinations of higher multipole fields have not been reported in the literature. Michaud et al. [19] investigated the bistable behavior in a linear quadrupole with a 4% added octopole field through fragmentation of reserpine ions induced by dipolar excitation. A plot of the precursor ion intensity versus excitation frequency (a "depletion peak") was expected to show bistable behavior on the low frequency side with excitation between the y rods (the larger rods), and bistable behavior on the high frequency side with excitation between the x rods (the smaller rods). However, bistable behavior was only observed with excitation between the y rods, while a relatively smooth and symmetric depletion curve was observed with excitation between the x rods. The higher order multipole amplitudes, though on the order of $A_2 \times 10^{-3}$ or less, were suspected of having non-negligible effects. In an effort to better understand these experimental observations, and in an effort to find combinations of multipoles that can provide bistable behavior, we have investigated the frequency shifts and resulting bistable behavior for quadrupoles that have added higher multipoles and combinations of higher multipoles.

We present a theoretical analysis of ion motion in a linear quadrupole ion trap incorporating one or more weak, even order, multipoles. The ions are excited by a dipole field and damped by collisions with a background gas. Because of the nonlinear fields, ion motions in the x and y directions are generally coupled. However the motions along the x and y axes are not coupled. We consider only ion motion along the x and y axes in a pseudopotential approximation. Collisions are modeled as a continuous drag force. A multiple time scales method is used to solve the equations of motion with a first order perturbation correction. Analytical relations between the oscillation amplitudes at steady state (the stationary amplitudes) and excitation frequency are calculated. The frequency response curves show that in some cases bistable behavior might be obtained, i.e., there are two stable amplitudes for a given excitation frequency.

2. Theory

2.1. Equations of motion

With higher multipoles, the motion of an ion in the potential given by Eq. (2) is very complex. We consider the ion motion in the effective, or time independent pseudopotential which derives from Eq. (2) which can be written as [31]:

$$V_{\text{eff}}(x_r, y_r) = \frac{ze}{4m\Omega^2}\left[\left(\frac{\partial\Phi(x_r, y_r)}{\partial x_r}\right)^2 + \left(\frac{\partial\Phi(x_r, y_r)}{\partial y_r}\right)^2\right]$$
$$= \frac{zeV_{\text{rf}}^2}{4\,m\Omega^2 r_0^2}\left[4A_2^2\frac{x_r^2 + y_r^2}{r_0^2} + 16A_2A_4\frac{x_r^4 - y_r^4}{r_0^4} + (16A_4^2 + 24A_2A_6)\frac{x_r^6 + y_r^6}{r_0^6} + \cdots\right] \quad (3)$$

where z is the number of charges on the ion, e is the electron charge, and m is the mass of the ion. With dipole excitation and damping due to collisions with the background gas, the equation of motion of an ion in the effective potential $V_{\text{eff}}(x_r, y_r)$ can be written as:

$$m\frac{\mathrm{d}^2\vec{r}}{\mathrm{d}t_r^2} = -ze\vec{\nabla}V_{\text{eff}}(x_r, y_r) - \Gamma\frac{\mathrm{d}\vec{r}}{\mathrm{d}t_r} + ze\vec{E}^{\mathrm{d}}\cos\omega_{\text{ex}}t_r, \quad (4)$$

where $\vec{r}$ is the ion position vector, $\vec{E}^{\mathrm{d}}$ is the electric field strength of the dipole excitation, $\omega_{\mathrm{ex}} = 2\pi f_{\mathrm{ex}}$ is the angular frequency of dipole excitation, and Γ is the damping coefficient which can be expressed as [19]

$$\Gamma = \frac{3.01\sigma n m_2 \sqrt{2k_{\mathrm{B}}T/m_2}}{2} \tag{5}$$

with σ the collision cross section of the ion, m_2 the mass of the buffer gas, n the number density of the background gas, k_{B} Boltzmann's constant, and T the gas temperature. Eq. (4) includes only the dipole excitation field (the dominant excitation field). A real rod set with additional higher multipoles will also have higher order multipole contributions to the excitation field.

Define $x = x_{\mathrm{r}}/r_0$, $y = y_{\mathrm{r}}/r_0$ as the dimensionless x and y coordinates, $t = \omega_0 t_r$ and $\omega = \omega_{\mathrm{ex}}/\omega_0$ as the dimensionless time and excitation frequency. Here ω_0 is the secular frequency in a pure quadrupole field given by

$$\omega_0 = 2\pi f_0 = \frac{qA_2}{\sqrt{8}}\Omega \tag{6}$$

where $q = 4zeV_{\mathrm{rf}}/m\Omega^2 r_0^2$ is a dimensionless Mathieu parameter.

Substituting these dimensionless variables into Eq. (4) and separating the quadrupole term from the higher multipoles gives the equations of motion of an ion along the x and y axes:

$$\frac{\mathrm{d}^2x}{\mathrm{d}t^2} + \lambda\frac{\mathrm{d}x}{\mathrm{d}t} + x + H_x(x) = \gamma_x\cos(\omega t) \tag{7}$$

$$\frac{\mathrm{d}^2y}{\mathrm{d}t^2} + \lambda\frac{\mathrm{d}y}{\mathrm{d}t} + y + H_y(y) = \gamma_y\cos(\omega t) \tag{8}$$

where the forms of the nonlinear functions $H_x(x)$ and $H_y(y)$ are determined by the higher multipoles present. The dimensionless damping constant λ and dipole excitation strengths γ_x and γ_y are defined as:

$$\lambda = \frac{\Gamma}{m\omega_0} = \frac{3.01\sigma P\sqrt{2m_2/k_{\mathrm{B}}T}}{2m\omega_0} \tag{9}$$

$$\gamma_x = \frac{ze}{m\omega_0^2 r_0}E_x^{\mathrm{d}} \approx \frac{zeA_{1x}V_{\mathrm{ex}}}{m\omega_0^2 r_0^2} \tag{10}$$

$$\gamma_y = \frac{ze}{m\omega_0^2 r_0}E_y^{\mathrm{d}} \approx \frac{zeA_{1y}V_{\mathrm{ex}}}{m\omega_0^2 r_0^2} \tag{11}$$

where P is the background gas pressure, A_{1x} and A_{1y} are constants which depend on the rod geometry, and V_{ex} is the zero to peak dipole excitation voltage (pole to ground).

2.2. Round rod quadrupoles with added octopole fields

Eqs. (7) and (8) are general forms for ion motion along the x and y axes when higher multipoles are added to the quadrupole field. Here we consider a quadrupole with an added octopole field used in our previous experimental investigations [19]. The ratio R_y/R_x ($R_x = r_0$) and multipole amplitudes up to and including A_{10} of this rod set are listed in Table 1. For such a quadrupole, for which the electrodes are symmetric about the x and y axes [20], the resulting multipoles are all even orders. As a result, the two nonlinear functions in Eqs. (7) and (8) take the following forms:

$$H_x(x) = B_3x^3 + B_5x^5 + B_7x^7 + B_9x^9 + B_{11}x^{11} + B_{13}x^{13} + \cdots, \tag{12a}$$

$$H_y(y) = -B_3y^3 + B_5y^5 - B_7y^7 + B_9y^9 - B_{11}y^{11} + B_{13}y^{13} + \cdots, \tag{12b}$$

where the coefficients are determined by the specific values of the multipoles,

$$B_3 = \frac{8A_2A_4}{A_2^2}, \tag{13a}$$

$$B_5 = \frac{12A_4^2 + 18A_2A_6}{A_2^2}, \tag{13b}$$

$$B_7 = \frac{48A_4A_6 + 32A_2A_8}{A_2^2}, \tag{13c}$$

$$B_9 = \frac{50A_2A_{10} + 45A_6^2 + 80A_4A_8}{A_2^2}, \tag{13d}$$

Table 1
The dimensionless multipole amplitudes A_n for a round rod quadrupole with 4.0% added octopole

R_y/R_x	A_0	A_2	A_4	A_6	A_8	A_{10}
1.516	−0.040366	1.0056	0.039889	−0.0029836	0.00085715	−0.0023215

Table 2
The nonlinear coefficients B_i for a quadrupole with a 4.0% added octopole field

B_3	B_5	B_7	B_9	B_{11}	B_{13}
0.317343	−0.0345241	0.0216271	−0.112330	−0.0113536	0.00151983

$$B_{11} = \frac{120A_4A_{10} + 144A_6A_8}{A_2^2}, \tag{13e}$$

$$B_{13} = \frac{210A_6A_{10} + 112A_8^2}{A_2^2}. \tag{13f}$$

For a quadrupole with 4.0% added octopole field (Table 1), these coefficients are listed in Table 2.

To investigate how the higher multipoles affect the ion motion, we keep only terms up to and including B_{13}. This cutoff is somewhat arbitrary. Substituting Eqs. (12a) and (12b) into Eqs. (7) and (8) yields the equations of motion for an ion in a quadrupole with even added multipole fields.

$$\frac{d^2x}{dt^2} + \lambda\frac{dx}{dt} + x + B_3x^3 + B_5x^5 + B_7x^7 + B_9x^9 + B_{11}x^{11} + B_{13}x^{13} = \gamma_x\cos(\omega t) \tag{14}$$

$$\frac{d^2y}{dt^2} + \lambda\frac{dy}{dt} + y - B_3y^3 + B_5y^5 - B_7y^7 + B_9y^9 - B_{11}y^{11} + B_{13}y^{13} = \gamma_y\cos(\omega t) \tag{15}$$

Note Eqs. (14) and (15) are nearly the same. They only differ in the signs of B_3, B_7, and B_{11}. Therefore, we solve and discuss the solutions of Eq. (14), and simply state those for Eq. (15) by changing the signs of the coefficients B_3, B_7, and B_{11}.

2.3. Solutions of the equations of motion

Eq. (14) is that of a damped nearly harmonic oscillator with nonlinear distortions to the force. No exact analytical solution can be found. An approximate solution can be found using perturbation methods. In order to properly order the terms in Eq. (14), we estimate the coefficients for our experiments, where $\Omega = 2\pi \times 7.68 \times 10^5$ rad/s, $r_0 = 4.5$ mm, $m/z = 609$, $A_2 \approx 1$ as in Table 1. For $q = 0.2$, the angular secular frequency given by Eq. (6) is

$$\omega_0 \approx 3.45 \times 10^5 \text{ rad/s} \tag{16}$$

For reserpine ions, the collision cross section is $\sigma = 280$ Å^2[32]. At a pressure $P = 1$ mTorr, or 0.27 Pa, with nitrogen as the collision gas, $m_2 = 28 \times 1.66 \times 10^{-27}$kg, and $T = 295$ K [19] Eq. (9) yields

$$\lambda \approx 7.69 \times 10^{-3} \ll 1 \tag{17}$$

For dipole excitation with $V_{ex} = 100$ mV, the excitation strength, defined by Eq. (10), is

$$\gamma_x = \gamma_y \approx 6.55 \times 10^{-3} \ll 1 \tag{18}$$

where for simplicity, we take $A_{1x} = A_{1y} = 1$.

Based on these estimates, Eq. (14) can be rewritten as

$$\frac{d^2x}{dt^2} + \varepsilon\lambda\frac{dx}{dt} + x + \varepsilon H_x(x) = \varepsilon\gamma_x\cos(\omega t) \tag{19}$$

where ε is of no physical meaning, and is only used to denote the order of the terms.

The perturbation method of multiple time scales is used to find an approximate solution for Eq. (19) [33,34]. In this method, two independently varying time scales are assumed. The fast time scale is the normal time $T_0 = t$, and the first order slow time scale is $T_1 = \varepsilon T_0$. Keeping only these two time scales we seek an approximate solution of the form

$$x = x(T_0, T_1) = x_0(T_0, T_1) + \varepsilon \cdot x_1(T_0, T_1) \tag{20}$$

Denote the time derivatives as $D_0 = d/dT_0$ and $D_1 = d/dT_1$. Inserting Eq. (20) into Eq. (19) and equating like terms according to the order of ε:

$$\varepsilon^0: \quad D_0^2x_0 + x_0 = 0 \tag{21}$$

$$\varepsilon^1: \quad D_0^2x_1 + x_1 = -2D_0D_1x_0 - \lambda D_0x_0 - H_x(x_0) + \gamma_x\cos(\omega T_0) \tag{22}$$

Eq. (21) is that of a simple harmonic oscillator with solution

$$x_0(T_0, T_1) = A(T_1)\cos(T_0 + \phi(T_1)) \tag{23}$$

where $A(T_1)$ and $\phi(T_1)$ are functions of the time scale T_1 and can be determined by removing secular terms in Eq. (22). For the near resonant excitation case, the excitation frequency is close to the secular frequency:

$$\omega = 1 + \varepsilon \cdot \Delta\omega_x \tag{24}$$

Substituting Eqs. (23) and (24) into the right hand side of Eq. (22), the following equation is obtained.

$$\begin{aligned}D_0^2x_1 + x_1 = {} & 2\frac{dA}{dT_1}\sin(T_0+\phi) + 2A\frac{d\phi}{dT_1}\cos(T_0+\phi) + \lambda A\sin(T_0+\phi) - \frac{B_3A^3}{4}[3\cos(T_0+\phi)+\cos 3(T_0+\phi)] \\ & - \frac{B_5A^5}{16}[10\cos(T_0+\phi)+5\cos 3(T_0+\phi)+\cos 5(T_0+\phi)] - \frac{B_7A^7}{64}[35\cos(T_0+\phi)+21\cos 3(T_0+\phi) \\ & +7\cos 5(T_0+\phi)+\cos 7(T_0+\phi)] - \frac{B_9A^9}{256}[126\cos(T_0+\phi)+84\cos 3(T_0+\phi)+36\cos 5(T_0+\phi) \\ & +9\cos 7(T_0+\phi)+\cos 9(T_0+\phi)] - \frac{B_{11}A^{11}}{1024}[462\cos(T_0+\phi)+330\cos 3(T_0+\phi) \\ & +165\cos 5(T_0+\phi)+55\cos 7(T_0+\phi)+11\cos 9(T_0+\phi)+\cos 11(T_0+\phi)] - \frac{B_{13}A^{13}}{4096}[1716\cos(T_0+\phi) \\ & +1287\cos 3(T_0+\phi)+715\cos 5(T_0+\phi)+286\cos 7(T_0+\phi)+78\cos 9(T_0+\phi)+13\cos 11(T_0+\phi)+\cos 13(T_0+\phi)] \\ & +\gamma_x\cos(T_0+\phi)\cos(\Delta\omega_x\cdot T_1-\phi) - \gamma_x\sin(T_0+\phi)\sin(\Delta\omega_x\cdot T_1-\phi) \end{aligned} \tag{25}$$

Setting coefficients of the terms $\cos(T_0+\phi)$ and $\sin(T_0+\phi)$ (the secular terms) to zero yields two differential equations:

$$2\frac{dA}{dT_1} + \lambda A = \gamma_x\sin(\Delta\omega_x\cdot T_1-\phi) \tag{26a}$$

$$2A\frac{d\phi}{dT_1} - \frac{3B_3}{4}A^3 - \frac{10B_5}{16}A^5 - \frac{35B_7}{64}A^7 - \frac{126B_9}{256}A^9 - \frac{462B_{11}}{1024}A^{11} - \frac{1716B_{13}}{4096}A^{13} = -\gamma_x\cos(\Delta\omega_x\cdot T_1-\phi) \tag{26b}$$

Let $\Psi = \phi - \Delta\omega_x T_1$, then $d\Psi/dT_1 = (d\phi/dT_1) - \Delta\omega_x$. For stationary solutions, neither the amplitude nor the phase should vary with time, i.e., $d\Psi/dT_1 = 0$ and $dA/dT_1 = 0$. Substituting these back into Eq. (26), we obtain a relation between the stationary amplitude (denoted A_e) and the frequency shift

$$\Delta\omega_{x\pm} = \pm\frac{1}{2}\sqrt{\left(\frac{\gamma_x}{A_e}\right)^2 - \lambda^2} + \frac{3B_3}{8}A_e^2 + \frac{10B_5}{32}A_e^4 + \frac{35B_7}{128}A_e^6 + \frac{126B_9}{512}A_e^8 + \frac{462B_{11}}{2048}A_e^{10} + \frac{1716B_{13}}{8192}A_e^{12} \tag{27}$$

where the subscripts $\pm$ corresponds to the $\pm$ signs in front of $\sqrt{(\gamma_x/A_e)^2-\lambda^2}$.

For the frequency shift to be real, the driving and damping have to satisfy,

$$\frac{\gamma_x}{A_e} \geq \lambda \tag{28}$$

It directly follows, that the maximum possible stationary amplitude is determined only by the ratio of the driving and damping strength for a given set of multipoles A_n.

$$A_{e\mathrm{Max}} = \frac{\gamma_x}{\lambda} \tag{29}$$

The frequency shift corresponding to $A_{e\mathrm{Max}}$ is determined by

$$\Delta\omega_{x\mathrm{Max}} = \frac{3B_3}{8}A_e^2 + \frac{5B_5}{16}A_e^4 + \frac{35B_7}{128}A_e^6 + \frac{126B_9}{512}A_e^8 + \frac{462B_{11}}{2048}A_e^{10} + \frac{1716B_{13}}{8192}A_e^{12} \tag{30}$$

3. Results and discussion

The plot of the stationary oscillation amplitude versus the excitation frequency, or its difference from the resonant frequency ω_0, is called the frequency response for given γ_x and λ [34]. For convenience we first find an equation for $d\omega/dA_e$. After rearranging terms, we square Eq. (27) and then take the derivative of ω with respect to the stationary amplitude A_e to obtain the following equation when $d\omega/dA_e = 0$:

$$\left(\frac{\gamma_x^2}{\lambda^2A_e^2} - 1\right)\left(\frac{3B_3}{2} + \frac{5B_5}{2}A_e^2 + \frac{105B_7}{32}A_e^4 + \frac{63B_9}{16}A_e^6 + \frac{1155B_{11}}{256}A_e^8 + \frac{1287B_{13}}{256}A_e^{10}\right)^2 - \frac{\gamma_x^4}{\lambda^2A_e^8} = 0 \tag{31}$$

3.1. A_2 plus one or more $A_{4n} \neq 0$

For a quadrupole incorporating a weak octopole field and no other multipoles, the only nonzero nonlinear terms are the terms with coefficients B_3 and B_5; all the other nonlinear terms have coefficients $B_{i>5} = 0$. The amplitude B_5 is about an order of magnitude smaller than B_3. For example, if $A_2 = 1.0$ and $A_4 = 0.04$, then $B_3 = 0.32$ and $B_5 = 0.0192$. In addition, B_5 is the coefficient of a higher order nonlinearity (x^5) which has the largest effect when the ion position $x \approx 1$. Ions inside a quadrupole have $x \leq 1$. Therefore, we may expect the cubic nonlinearity to dominate. This results in a case similar to that of a cubic nonlinearity only, as in Refs. [22,34].

For given driving and damping forces, the shape of the frequency response curve depends on the sign and magnitude of the nonlinearity. Fig. 1 shows the frequency response curves for various amounts of added octopole field. The parameters Ω and r_0 are chosen to match those used in our experiments. The ion is protonated reserpine ($m/z = 609$).

When the nonlinearity is zero, the frequency response curve is centered at the resonant frequency ω_0, and the relation between A_e and ω (or f) is single-valued. In the presence of the nonlinearity, the frequency response bends away from that with no nonlinearity; the higher

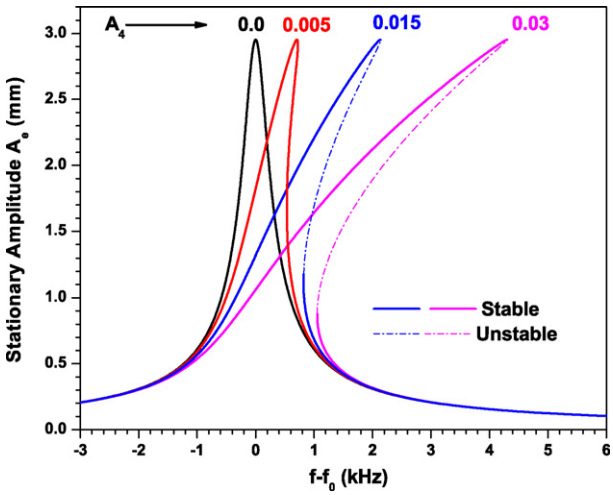

Fig. 1. Frequency response with multipole amplitudes $A_2 = 1.0$, $A_4 = 0.000, 0.005, 0.015, 0.030$, and all the other $A_n = 0.0$. $A_{1x} = 1.0$, $P = 1.0$ mTorr, $V_{ex} = 153$ mV, $f_0 = 54.323$ kHz, and $q = 0.20$.

the nonlinearity, the greater the bending. This bending of the frequency response results in a multivalued dependence of the stationary amplitude A_e on the resonant frequency, for instance, when $A_4 = 0.030$ and $f - f_0 \geq 1.05$ kHz. However, not all the stationary amplitudes are stable. The stability of the A_e can be determined by analyzing the eigenvalues of the Jacobian matrix of Eq. (26) for each of the (A_e, f) pairs [35]. Usually this can be done for each of the branches of the frequency response curve. When one or more of the eigenvalues has a positive real part, the solution is unstable, otherwise stable. In Fig. 1, for the curves with $A_4 = 0.015$ and 0.030 only, the stable and unstable solutions are indicated by the solid and dash dot lines, respectively. *Bistable* behavior can arise for frequencies for which there are two stable stationary amplitudes.

The direction that the frequency response curve bends depends on the sign of the nonlinearity. Fig. 2(a) shows the relation of the stationary amplitude versus the shift from the secular frequency for a quadrupole with $A_4 = 0.04$. The responses for both the x and y directions are plotted. Recall from Eq. (12a) and (12b) the nonlinearities are $+B_3$ and $-B_3$ for the x and y directions, respectively. It is also apparent from Fig. 2(a), for a quadrupole with A_2 and A_4 only, the frequency response curves in the x and y directions are nearly mirror images. Note both the nonzero terms B_3 and B_5 are included. As mentioned earlier, the influence of the term B_5 is very small. For these conditions, when $A_e = 0.5$, the term in B_5 contributes only about 1% of the frequency shift. For comparison Fig. 2(b) illustrates the frequency response of a quadrupole with $A_2 = 1.0$ and $A_8 = 0.04$ only. The main difference between the influence of A_4 and A_8 is that the presence of A_8 is only observed at larger oscillation amplitudes. This is to be expected for a higher order nonlinearity. For the same amount of nonlinearity, driving, and damping, the frequency range for which bistability occurs is smaller for the A_2, A_8 only quadrupole.

The effect of damping for a given dipole excitation amplitude is illustrated in Fig. 3, which shows the frequency response for different pressures of the background gas. There is a minimum damping, related to the excitation strength, required for the occurrence of bistable behavior. For instance, $V_{ex} = 30$ mV is insufficient to give bistable behavior at 1 mTorr. At a lower pressure the same excitation amplitude gives bistable behavior. The smaller the damping, the larger the maximum stationary amplitude, and the wider the frequency range over which bistability may occur. The width of the response curve does not vary much over this range of pressures.

The effect of excitation amplitude at a pressure of 0.2 mTorr is illustrated in Fig. 4. Increasing excitation strength for a given damping has an effect similar to decreasing damping for a given excitation strength. The main difference lies in the more rapid increase in the width of the frequency response curve for smaller A_e. For instance, when the excitation amplitude is increased from $V_{ex} = 30$ mV to $V_{ex} = 60$ mV (a factor of two), the change of the frequency response width is much larger than when the pressure was reduced from 1 mTorr to 0.5 mTorr (a factor of two). This is the result of the term $\sqrt{\gamma_x^2/A_e^2 - \lambda^2}$. For $A_e < 1$, the driving term γ_x is multiplied by a factor $1/A_e > 1$.

The occurrence of bistability for a given set of parameters is indicated by the bending of the frequency response curve. Since at the bending points the condition $d\omega/dA_e = 0$ holds, the minimum excitation voltage required for bistability can be derived from Eq. (31). In general, if there is a real solution to Eq. (31), bistability occurs. In the case of A_2 and A_4 only, neglecting B_5, Eq. (31) simplifies to

$$g(\zeta) = \zeta^4 - C_{B_3}\zeta + C_{B_3} = 0, \tag{32}$$

where

$$\zeta = \frac{\gamma_x^2}{\lambda^2 A_e^2} = \left(\frac{A_{e\mathrm{Max}}}{A_e}\right)^2 \tag{33}$$

and therefore $\zeta \geq 1$, and

$$C_{B_3} = \frac{9\gamma_x^4 B_3^2}{4\lambda^6} > 0 \tag{34}$$

where C_{B_3} is a constant determined by the added octopole amplitude, the dipole excitation strength, and the damping strength. The nonlinear resonance causes bistability if there is a root to Eq. (32).

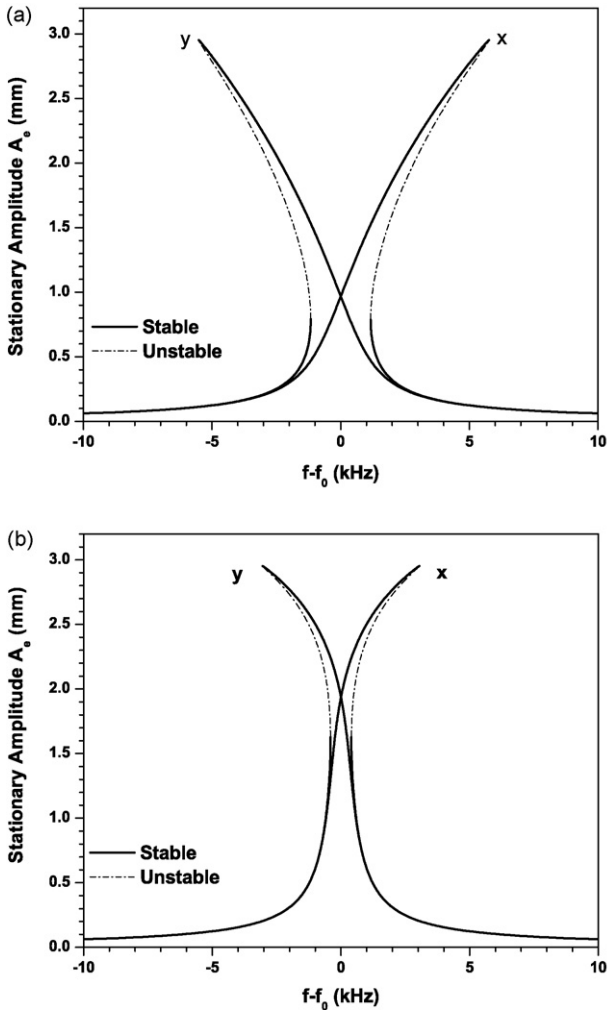

Fig. 2. Frequency response curves with (a) $A_2 = 1$, $A_4 = 0.04$, and all the other $A_n = 0$; (b) $A_2 = 1$, $A_8 = 0.04$, and all the other $A_n = 0$. Both are calculated for $q = 0.20$, $P = 1$ mTorr, $V_{ex} = 153$ mV, and $f_0 = 54.323$ kHz. All the nonzero coefficients B_i are included.

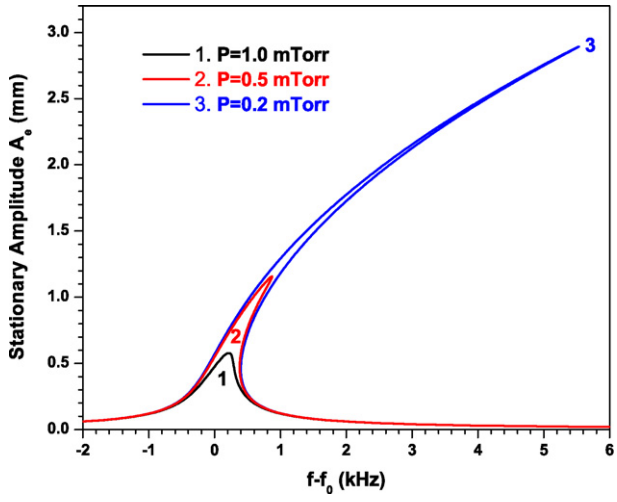

Fig. 3. Frequency response curves of a quadrupole with $A_2 = 1.0$, $A_4 = 0.04$, and all the other $A_n = 0$ at different pressures with $V_{ex} = 30$ mV, $f_0 = 54.323$ kHz.

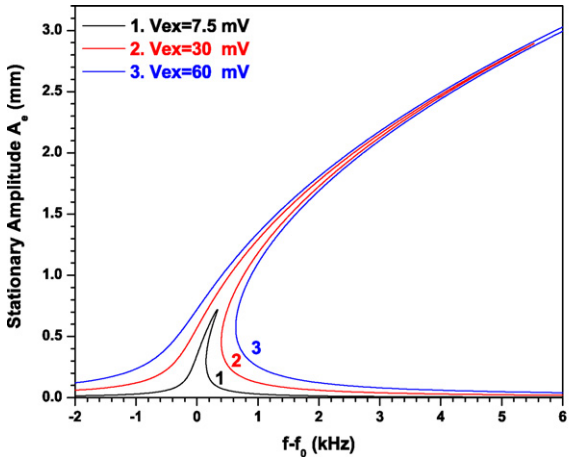

Fig. 4. Frequency response curves of a quadrupole with $A_2 = 1.0$, $A_4 = 0.04$, and all the other $A_n = 0$ for different excitation amplitudes. $P = 0.2$ mTorr, $V_{ex} = 7.5$, 30, and 60 mV, and $f_0 = 54.323$ kHz.

The equation

$$\frac{\mathrm{d}g(\zeta)}{\mathrm{d}\zeta} = 4\zeta^3 - C_{B_3} = 0 \tag{35}$$

gives a local extremum of $g(\zeta)$ at $\zeta_m = \sqrt[3]{C_{B_3}/4} > 0$; and since $\mathrm{d}g^2(\zeta_m)/\mathrm{d}\zeta^2 > 0$, we get a minimum $g_{\min}(\zeta_m)$.

Asymptotically, $g(\zeta_{\min} = 1) = 1$, and $g(\zeta \to \infty) \approx \zeta^4 > 0$. It can be concluded that there will be roots to Eq. (32) if $g_{\min}(\zeta_m) < 0$. In order for the frequency response curve to bend, $g_{\min}(\zeta_m) \geq 4/3$ has to hold, or equivalently

$$\sqrt[3]{\frac{C_{B_3}}{4}} = \sqrt[3]{\frac{9\gamma_x^4 B_3^2}{16\lambda^6}} \geq \frac{4}{3}. \tag{36}$$

Using the parameters as defined in Eqs. (9) and (10) and taking the equal sign from the above equation, the critical condition for bistability can be obtained

$$V_{B_3,\min} = r_0 E_c^{\mathrm{d}} \tag{37a}$$

$$V_{B_3,\min} = \left(\frac{4}{9\sqrt{3}}\right)^{1/2} \lambda^{3/2} \left(\frac{A_2}{A_4}\right)^{1/2} \frac{m r_0^2 \omega_0^2}{z e A_{1x}} \tag{37b}$$

where eE_c^{d} stands for the critical dipole driving force to give bistability for a given set of quadrupole and added octopole fields with damping. Note Eq. (37) coincides with that given by Landau and Lifshitz [22], and further discussed by Michaud et al. [19]. The frequency shift at the critical point is

$$\omega_c = \pm\sqrt{\frac{3B_3}{4}} A_c = \pm\frac{9}{64}\frac{\gamma_x^2}{\lambda^2} B_3 \tag{38}$$

For the case of $A_2 = 1.0$ and $A_4 = 0.04$ only, for a reserpine ion ($m/z = 609$) collisionally cooled by 2 mTorr N_2 at $T = 295$ K, with $q = 0.20$, then $V_{B_3,\min} \approx 73/A_{1x}$ mV, zero to peak and pole to ground.

It is readily deduced that for a quadrupole with weak multipoles A_{4n} only, because of the resulting opposite signs in front of the nonzero coefficients B_3, B_5, and B_7 for the x and y directions, the frequency response curves are mirror images for the x and y directions, as is the resulting bistable behavior. However, this does not mean the frequency response curves, caused by different nonlinear terms, bend in the same direction. The bending direction is determined by the signs and magnitudes of each of the terms B_i. Fig. 5 shows an example. In Fig. 5(a), A_4 and A_8 have the same sign and the nonlinear terms B_3 and B_7 have the same sign. Both the A_4 and A_8 terms cause the frequency response curves to bend to the higher/lower frequency side for the x/y direction. In Fig. 5(b) $A_8 < 0$, so the terms B_3 and B_7 have opposite signs. When the oscillation amplitude is small, the frequency response curve first bends in the direction determined by the term A_4; then at higher oscillation amplitudes it turns around and bends in the opposite direction because of the 16-pole term A_8. When the A_{4n} have the same sign, the higher multipoles all cause frequency shifts in the same direction and reinforce the effects of each other, as in Fig. 5(a). Here all the multipoles produce a shift to higher frequency for the x motion and to lower frequency for the y motion. When some of the higher A_{4n} differ in sign, the different multipoles produce shifts of opposite sign for excitation in a given direction, and to some extent counteract the effects of each other, as in Fig. 5(b). This reduces the range of frequencies and operating conditions over which bistable behavior might be obtained. Thus to produce bistable behavior on both the low and high frequency sides of a response curve, quadrupoles with $A_{4n} \neq 0$ and all the A_{4n} of the same sign might be preferred.

A quadrupole with A_2 and one or more of $A_{4n} \neq 0$ can always be constructed from electrodes that have surfaces determined by

$$A_2(x^2 - y^2) + \sum_{n=1}^{N} A_{4n}\phi_{4n} = \pm 1, \tag{39}$$

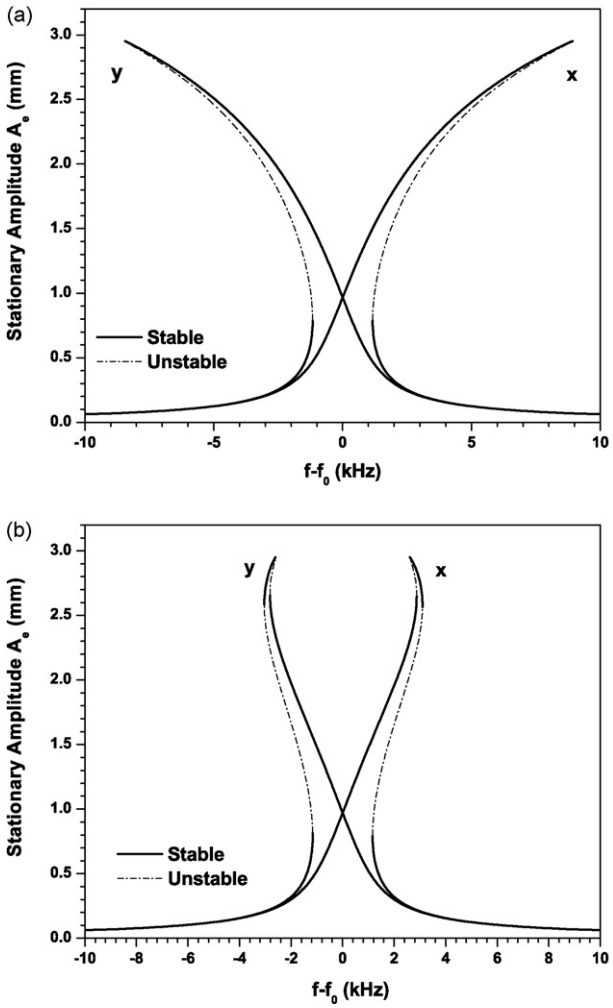

Fig. 5. Frequency response curves with (a) $A_2 = 1$, $A_4 = 0.04$, $A_8 = 0.04$, and all other $A_n = 0$; (b) $A_2 = 1$, $A_4 = 0.04$, $A_8 = -0.04$, and all other $A_n = 0$. Both are calculated for $q = 0.20$, $P = 1$ mTorr, $V_{ex} = 153$ mV, and $f_0 = 54.323$ kHz. All the nonzero coefficients B_i are included.

where ϕ_{4n} can be found from Eq. (1).

3.2. A_2 plus one or more $A_{4n+2} \neq 0$ only

The general effect of damping and excitation strength on the frequency response for A_2 and one or more $A_{4n} \neq 0$ in Section 3.1 applies to quadrupoles with A_2 and one or more $A_{4n+2} \neq 0$. The main difference for a quadrupole incorporating one or more A_{4n+2} is that the frequency response curves for the x and y directions are identical. The direction that the frequency response curves bend is determined by the signs of the nonlinear coefficients B_i. Fig. 6(a) shows a response curve of a quadrupole with A_2 and $A_6 \neq 0$; while Fig. 6(b) an example of a quadrupole with A_2 and $A_{10} \neq 0$ and all the other $A_n = 0$. In this case bistable behavior might be obtained, but only on one side of the frequency response curve.

As with a quadrupole with only an added octopole field, the minimum excitation voltage required for bistability to occur for a quadrupole with A_2 and a small amount of A_6 only can be derived as follows. In this case $B_5 \neq 0$, all the other coefficients B_i are negligible or zero, and Eq. (31) becomes

$$g(\zeta) = \zeta^6 - C_{B_5}\zeta + C_{B_5} = 0 \tag{40}$$

where ζ is the same as in Eq. (33), and the constant C_{B_5} is

$$C_{B_5} = \frac{25B_5^2}{4}\frac{\gamma_x^8}{\lambda^{10}} \tag{41}$$

By definition, $\zeta \in (\zeta_{\min} = 1, \zeta_{\max} = +\infty)$ and

$$g(\zeta_{\min}) = 1 > 0 \tag{42a}$$

asymptotically

$$g(+\infty) \propto \zeta^6 > 0 \tag{42b}$$

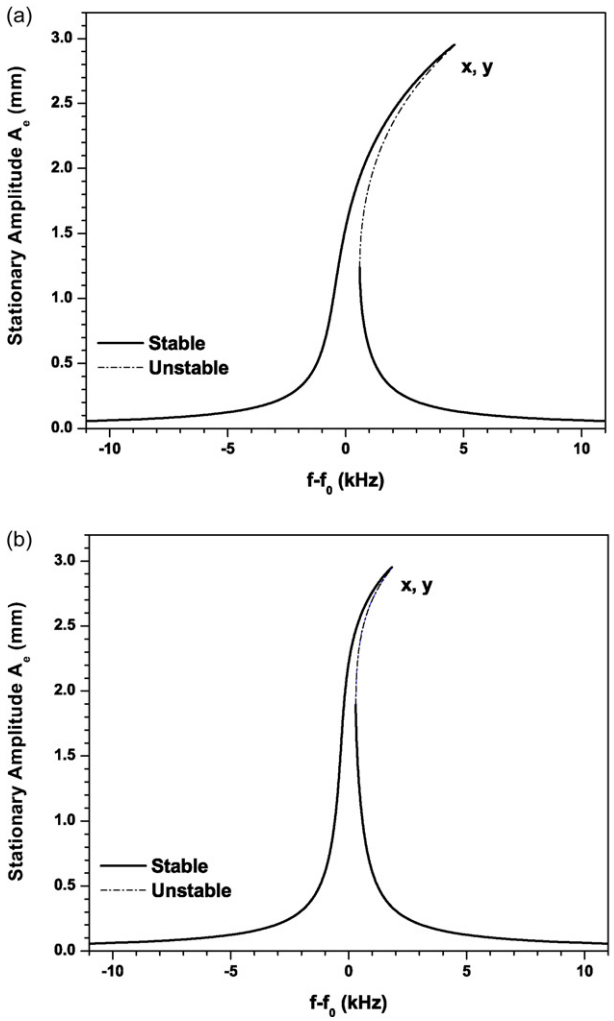

Fig. 6. Frequency response curves with (a) $A_2 = 1$, $A_6 = 0.04$, and all other $A_n = 0$; (b) $A_2 = 1$, $A_{10} = 0.04$, and all other $A_n = 0$. Both are calculated for $q = 0.20$, $P = 1$ mTorr $V_{ex} = 153$ mV, and $f_0 = 54.323$ kHz. All the nonzero coefficients B_i are included. The frequency response curves for the x and y directions are identical.

In order for a root of Eq. (40) to exist, there has to be at least one local negative extremum for the function of $g(\zeta)$ as in Eq. (40). To find the conditions for such a local extremum, letting

$$\frac{dg(\zeta)}{d\zeta} = 0, \tag{43}$$

yields a single local extremum at $\zeta_m = (C_{B_5}/6)^{1/5}$; and since at this extremum $g(\zeta_m) = C_{B_5}[1 - (5/6)(C_{B_5}/6)^{1/5}] \leq 0$ has to hold, it yields the condition

$$\left(\frac{C_{B_5}}{6}\right)^{1/5} \geq \frac{6}{5}. \tag{44}$$

Furthermore, as the only local extremum, taking into consideration the asymptotic behavior, it will have to be a minimum. This translates into letting

$$\frac{d^2 g(\zeta_m)}{d\zeta^2} = 30\left(\frac{C_{B_5}}{6}\right)^{4/5} \geq 0, \tag{45}$$

Since this is always true, ζ_m must be a negative local minimum.

In short, Eq. (44) is the condition for the occurrence of bistability. Using the parameters defined in Eqs. (9)–(11) and taking the equal sign, the minimum excitation voltage required for bistability to occur is

$$V_{B_5,\min} = r_0 E_c^d \tag{46a}$$

$$V_{B_5,\min} = \frac{2}{5}\left(\frac{45}{4}\right)^{1/8} \lambda^{5/4} \left(\frac{A_2}{A_6}\right)^{1/4} \frac{m r_0^2 \omega_0^2}{z e A_{1x}} \tag{46b}$$

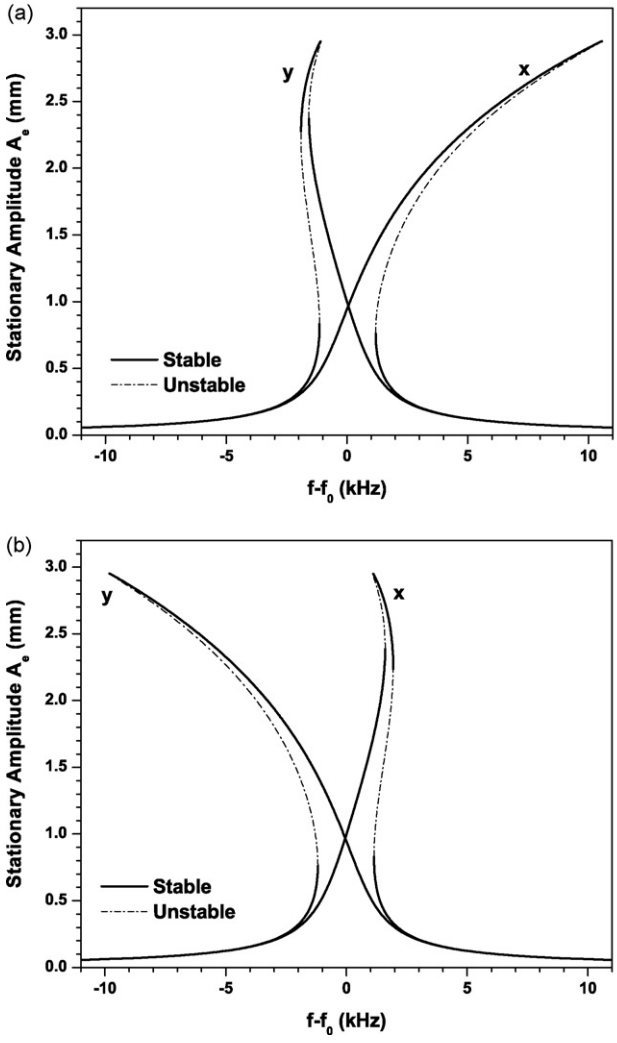

Fig. 7. Frequency response curves with (a) $A_2 = 1, A_4 = 0.04, A_6 = 0.04$, and all the other $A_n = 0$; (b) $A_2 = 1, A_4 = 0.04, A_6 = -0.04$, and all the other $A_n = 0$. Both are calculated for $q = 0.20$, $P = 1$ mTorr, $V_{ex} = 153$ mV, and $f_0 = 54.323$ kHz.

For the case of $A_2 = 1.0$ and $A_6 = 0.04$ only, for reserpine ions ($m/z = 609$) collisionally cooled by 2 mTorr N_2 at $T = 295$ K, and with $q = 0.20$, then $V_{B_5,\min} \approx 100/A_{1x}$ mV, zero to peak and pole to ground. This value is larger than that of the case of A_2 and A_4 only with the same operating conditions. The higher excitation voltage required to produce bistability is characteristic of a higher order nonlinear process.

3.3. Round rod quadrupoles

With both $A_{4n} \neq 0$ and $A_{4n+2} \neq 0$, the frequency responses are asymmetric in the x and y directions. This is shown in Fig. 7(a), where A_4 and A_6 are the same sign, and Fig. 7(b), where A_4 and A_6 have opposite signs.

For a quadrupole with an added octopole field constructed from round rods, the dominating higher order multipole is the octopole (Table 1). If the effects of the higher multipoles with much smaller A_n can be neglected, symmetric responses for the x and y directions are expected (like a quadrupole with only $A_2 \neq 0$ and $A_4 \neq 0$). However this is not generally the case. Calculated response curves for a quadrupole with 4% added octopole and the multipole amplitudes of Table 1 are shown in Fig. 8. Since the y rods are larger than the x rods, when the same excitation voltage is applied, slightly different excitation strengths are seen by the ions. From the different frequency response curves for the x and y directions, it is clear the effects of the higher order multipoles are not negligible in this case. Because the maximum oscillation amplitudes (ca. 4.5 mm) are near r_0, the higher multipoles influence the ion motion. Calculated response curves for the experiment of Michaud et al. [19] are shown in Fig. 9. Here the maximum oscillation amplitudes (ca. 2.4 mm) are substantially lower than r_0, and the curves for the x and y directions are approximately symmetric. Despite these curves, the experiments showed bistable behavior (or at least strongly asymmetric depletion peaks) with excitation in y, but not in x. Thus these calculations of the stationary amplitudes are not, in themselves, sufficient to predict the occurrence of bistable behavior in a given experiment. Where there are two stable solutions for the oscillation amplitude at a give excitation frequency, the initial conditions and dynamics of the ion motion will determine the stationary amplitudes of an ion. For an ensemble of ions with a distribution of initial conditions, the effects of the bistable behavior of individual ions may not be seen.

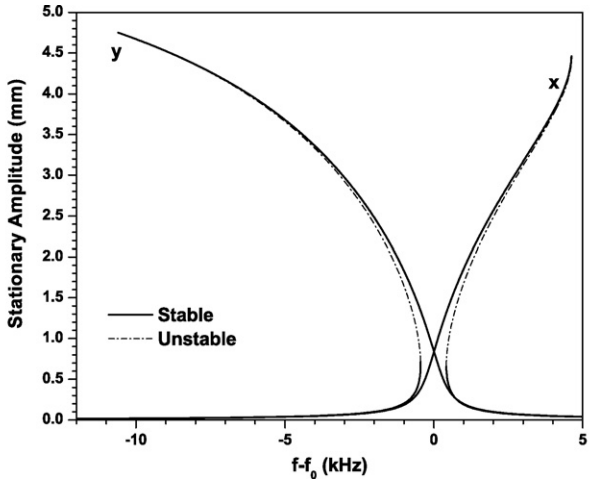

Fig. 8. Frequency response curves for a round rod quadrupole with 4% added octopole field, with $q = 0.20$, $P = 0.2$ mTorr, $V_{ex} = 30$ mV, $A_{1x} = 0.775$, $A_{1y} = 0.826$, and $f_0 = 54.959$ kHz.

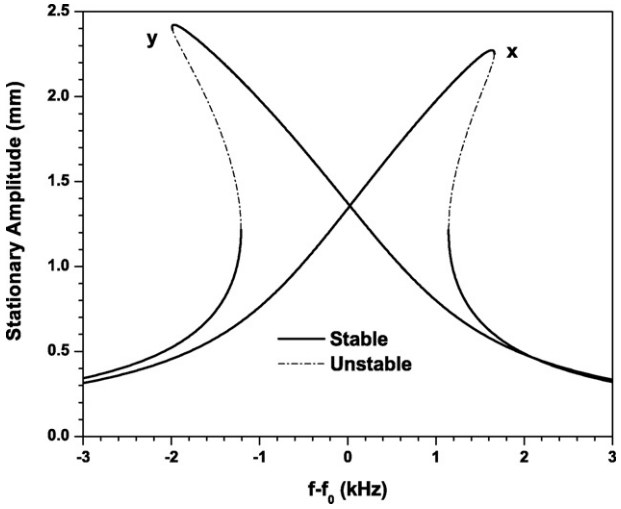

Fig. 9. Frequency response curves for a round rod quadrupole with 4% added octopole field, with $q = 0.20$, $P = 2.0$ mTorr, $V_{ex} = 153$ mV, $A_{1x} = 0.775$, $A_{1y} = 0.826$, and $f_0 = 54.959$ kHz.

4. Summary

The method of multiple time scales has been used to calculate frequency response curves for ions with dipole excitation in linear quadrupoles with small amounts of higher multipoles added to the potential. Ion motion along the x axis ($y = 0$) and y axis ($x = 0$) is calculated within the pseudopotential approximation. Multipoles up to $n = 10$ (the twenty pole term) were included in the calculation, but the method could be extended to include higher multipoles. The method could also be used to calculate frequency response curves for ion motion in other geometry ion traps, for example, truncated 3D hyperbolic, rectilinear, cylindrical, and halo ion traps.

The calculations show that the effects of higher order multipoles with amplitudes $A_2 \times 10^{-3}$ are non-negligible. In some cases there is more than one solution for the stationary amplitude at a given excitation frequency, so that bistable behavior might be seen. To produce bistable behavior on both the low and high frequency sides of a response curve, in order to provide a method for isolating ions with high mass resolution, a quadrupole with multipoles $A_{4n} \neq 0$ with all A_{4n} of the same sign is preferred. In this case the higher multipoles all cause frequency shifts in the same direction; for example to higher frequency for the x motion and to lower frequency for the y motion when the $A_{4n} > 0$. Conversely a quadrupole with only multipoles $A_{4n+2} > 0$ has frequency shifts in the same directions for both the x and y motions, and so will not produce bistable behavior on both the low and high frequency sides of a response curve. Comparison of calculated response curves of a round rod quadrupole with 4% added octopole field to experiments by Michaud et al. [19] shows that even when the response curves show possible bistable behavior, such behavior may not be seen in experiments. Detailed consideration of the dynamics and initial conditions of the ions may be necessary.

To more directly probe response curves for these nonlinear resonances it is beneficial to use a non-destructive method such as laser induced fluorescence of atomic ions, as in Ref. [36]. Because atomic ions do not fragment, the interpretation of the experiments is more straightforward. Such experiments might also be used to investigate hysteresis effects [9,33,34] in the response curves.

Acknowledgments

This work was supported by the Natural Sciences and Engineering Research Council and MDS Sciex through an Industrial Research Chair.

References

[1] W.R. Smythe, Static and Dynamic Electricity, McGraw Hill Book Company, New York, 1939, p. 62.
[2] M. Szilagyi, Electron and Ion Optics, Plenum Press, New York, 1988.
[3] J. Franzen, Int. J. Mass Spectrom. Ion Proc. 125 (1993) 165.
[4] J.E.P. Syka, Practical Aspects of Ion Trap Mass Spectrometry, vol. 1, CRC Press, Boca Raton, FL, 1995 (Chapter 4), p. 169.
[5] Y. Wang, J. Franzen, Int. J. Mass Spectrom. Ion Proc. 112 (1992) 167.
[6] Y. Wang, J. Franzen, Int. J. Mass Spectrom. Ion Proc. 132 (1994) 155.
[7] M. Sudakov, Int. J. Mass Spectrom. 206 (2001) 27.
[8] N. Rajanbabu, A. Marathe, A. Chatterjee, A.G. Menon, Int. J. Mass Spectrom. 261 (2007) 170.
[9] A.A. Makarov, Anal. Chem. 68 (1996) 4257.
[10] Z. Ouyang, G. Wu, Y. Song, H. Li, W.R. Plass, R.G. Cooks, Anal. Chem. 76 (2004) 4595.
[11] G. Wu, R.G. Cooks, Z. Ouyang, Int. J. Mass Spectrom. 241 (2005) 119.
[12] D.E. Austin, M. Wang, S.E. Tolley, J.D. Maas, A.R. Hawkins, A.L. Rockwood, H.D. Tolley, E.D. Lee, M.L. Lee, Anal. Chem. 79 (2007) 2927.
[13] J. Schulte, P.V. Shevchenko, A.V. Radchik, Rev. Sci. Instrum. 70 (1999) 3566.
[14] D.J. Douglas, N.V. Konenkov, Rapid Commun. Mass Spectrom. 16 (2002) 1425.
[15] I.E. Dayton, F.C. Shoemaker, R.F. Mozley, Rev. Sci. Instrum. 25 (1954) 485.
[16] J. Franzen, R.H. Gabling, M. Schubert, Y. Wang, Practical Aspects of Ion Trap Mass Spectrometry, vol. 1, CRC Press, Boca Raton, FL, 1995 (Chapter 3), p. 49.
[17] B.A. Collings, W.R. Stott, F.A. Londry, J. Am. Soc. Mass Spectrom. 14 (2003) 622.
[18] B.A. Collings, J. Am. Soc. Mass Spectrom. 16 (2005) 1342.
[19] A.L. Michaud, A.J. Frank, C. Ding, X. Zhao, D.J. Douglas, J. Am. Soc Mass Spectrom. 16 (2005) 835.
[20] M. Sudakov, D.J. Douglas, Rapid Commun. Mass Spectrom. 17 (2003) 2290.
[21] N. Konenkov, F. Londry, C. Ding, D.J. Douglas, J. Am. Soc. Mass Spectrom. 17 (2006) 1063.
[22] L.D. Landau, E.M. Lifshitz, Mechanics, Pergamon Press, New York, 1960, p. 74.
[23] N.W. McLachlan, Ordinary Non-linear Differential Equations in Engineering and Physical Sciences, Oxford University Press, London, 1956, p. 57.
[24] N. Rajanbabu, A. Chatterjee, A.G. Menon, Int. J. Mass Spectrom. 261 (2007) 159.
[25] L. Ding, M. Sudakov, F.L. Brancia, R. Giles, S. Kumashiro, J. Mass Spectrom. 39 (2004) 471.
[26] R.E. March, M.R. Weir, M. Tkaczyk, F.A. Londry, R.L. Alfred, A.M. Franklin, J.F.J. Todd, Organic Mass Spec. 28 (1993) 499.
[27] J.D. Williams, K.A. Cox, R.G. Cooks, S.A. McLuckey, K.J. Hart, D.E. Goeringer, Anal Chem. 66 (1994) 725.
[28] M. Splendore, F.A. Londry, R.E. March, R.J.S. Morrison, P. Perrier, J.A. Andre, Int. J. Mass Spectrom. Ion Proc. 156 (1996) 11.
[29] M. Nappi, V. Frankevich, M. Soni, R.G. Cooks, Int. J. Mass Spectrom. 177 (1998) 91.
[30] S. Sevugarajan, A.G. Menon, Int. J. Mass Spectrom. 189 (1999) 53.
[31] H.G. Dehmelt, Adv. Atom. Mol. Phys. 3 (1967) 53.
[32] G. Javahary, B.A. Thomson, J. Am. Soc. Mass Spectrom. 8 (1997) 697.
[33] J.J. Thomsen, Vibrations and Stability, 2nd ed., Springer, Berlin, 2003, p. 88.
[34] A.H. Nayfeh, D.T. Mook (Eds.), Nonlinear Oscillations, John Wiley and Sons, New York, 1979, p. 161 (Chapter 4).
[35] J.J. Thomsen, Vibrations and Stability, 2nd ed., Springer, Berlin, 2003, p. 77.
[36] A. Drakoudis, M. Sollner, G. Werth, Int. J. Mass Spectrom. 252 (2006) 61.